Self archive of H. Torii, *J. Chem. Phys.* **127** (5), 054508 (2007)

Scheme of detecting microscopic inhomogeneity in binary liquid mixtures utilizing resonantly coupled vibrational modes

Hajime Torii [a)]

Department of Chemistry, School of Education, Shizuoka University,
836 Ohya, Shizuoka 422-8529, Japan

[a)] Telephone and Fax: +81-54-238-4624; E-mail: torii@ed.shizuoka.ac.jp.

Influence of microscopic inhomogeneity in binary liquid mixtures on their vibrational spectra is studied by doing calculations on a model liquid system. The concentration dependence of the noncoincidence effect (NCE), which is a feature of vibrational bands related to intermolecular resonant coupling of vibrational modes, is analyzed. It is suggested that observation of convex behavior of the NCEs for the vibrational bands of both species, especially that of the less polar species, in a binary liquid mixture is an indication of the occurrence of microscopic inhomogeneity.

I. INTRODUCTION

Microscopic structural ordering in binary liquid mixtures is a fundamental problem in liquid state chemistry and physics, for better understanding of intermolecular interactions and, in particular, of molecular self organization on the microscopic scale. Sometimes this problem has been discussed in relation to thermodynamic properties. It is known that the thermodynamic properties of many real liquid mixtures deviate more or less from those of ideal mixtures,[1] and some of those deviations are referred to as anomalous. Based on the Kirkwood–Buff theory,[2,3] those anomalous thermodynamic properties are related[4] to microscopic inhomogeneity (or microheterogeneity[5]) of liquid structures, which means preferential solvation by the molecules of the same species within a length scale of a multiple of molecular diameters in binary liquid mixtures,[6] originating from molecular self association of moderate strength (not at all weak, but not so strong to lead to macroscopic phase separation). In some recent studies, the intermolecular interactions and the liquid structures are more directly analyzed by using the small- and large-angle x-ray and neutron scattering methods,[7–11] the vibrational [infrared (IR) and Raman], dielectric, and nuclear magnetic resonance (NMR) spectroscopic methods,[12–17] and the molecular dynamics (MD) simulation and other theoretical methods.[16–19] While small-angle x-ray and neutron scattering measurements lead to estimates of the Debye correlation lengths of liquid structures,[7–9] more molecularly detailed information is derived by the large-angle x-ray and neutron diffractions, the vibrational and NMR spectroscopic methods, and the computational and theoretical methods. However, for example in the case of the methanol/water binary liquid mixture, there is a contradiction among the results of the studies utilizing these methods; no signature of microscopic inhomogeneity has been found in the low-frequency Raman spectrum,[20] as also supported by x-ray diffraction[21] and thermodynamic studies,[1] but the occurrence of substantial molecular segregation has been suggested in a neutron diffraction study.[22] In this sense, further methodological development is preferable to obtain clearer knowledge on the intermolecular interactions and liquid structures.

In the previous studies on the vibrational spectra in the 4000–700 cm^{-1} region focusing on the microscopic inhomogeneity of binary liquid mixtures,[12,13] vibrational frequency shifts induced by the surrounding molecules have been analyzed. Based on the classification of the effects of intermolecular interactions on the vibrational spectra introduced in our previous study,[23–26] this quantity is classified as *diagonal*, meaning that it

is a property of individual molecules affected by their local environment, such as dielectric reaction field and hydrogen bonding. However, there is another category of phenomena originating from an *off-diagonal* property of molecular vibrations, meaning that it is related to direct intermolecular coupling of vibrational modes. The noncoincidence effect (NCE), which is the phenomenon that the frequency positions of the IR, isotropic Raman, and anisotropic Raman components of a vibrational band do not coincide,[23–31] belongs to this category. This effect is seen in liquid systems as well as in biomolecules with repeat units,[32,33] and is most clearly recognized in the resonant case, where the intrinsic frequencies of the coupled modes are sufficiently close to each other as compared with the magnitude of the coupling. As a result, in binary liquid mixtures, this effect originates almost exclusively from the vibrational couplings between molecules of the same species, and diminishes even upon dilution with an isotopically substituted species, for example, upon dilution of acetone-^{12}C=O with acetone-^{13}C=O.[31] Its concentration dependence is affected by details of liquid structural changes, such as the anisotropy in the liquid structural changes in methanol/CCl_4.[30] In this sense, analysis of this effect is expected to be useful also to detect microscopic inhomogeneity of liquid structures as a property related to the distances and relative orientations of the molecules of the same species.

In the present work, this point is studied by doing calculations on a model liquid system. The effect of preferential solvation on vibrational band profiles is examined by isolating it from those of other factors of liquid structures. It is shown that a nonlinear convex behavior of the concentration dependence of the NCEs of the vibrational bands of both species (not only one of those species) in a binary liquid mixture is an indication of the occurrence of microscopic inhomogeneity. Distinction with the nonlinear concentration dependence of the NCEs arising from polarity difference is discussed.

II. MODEL AND COMPUTATIONAL PROCEDURE

The model liquid system adopted in the present work consists of polar spherical particles interacting with each other by the Lennard-Jones and dipole–dipole interactions (Stockmayer fluid),[34] with a one-dimensional oscillator (representing a vibrational degree of freedom) having a vibrational transition dipole and a Raman tensor being buried in each particle.[35] Denoting the coordinate (weighted by the square root of the reduced mass) of the mth particle's oscillator as q_m, its vibrational transition dipole and Raman tensor are expressed within the harmonic approximation as $(\partial \boldsymbol{\mu}_m/\partial q_m) \langle 1_m| q_m |0_m\rangle$ and $(\partial \boldsymbol{\alpha}_m/\partial q_m) \langle 1_m| q_m |0_m\rangle$, respectively, where $|0_m\rangle$ and $|1_m\rangle$ are the ground and one-quantum excited states of this oscillator. While the Lennard-Jones and dipole–dipole interaction parameters were assumed to be the same for all the particles (ε = 150 K, σ = 4.2 Å, and $\mu^* \equiv \mu(\varepsilon\sigma^3)^{1/2} = 2.5$),[35] two sets of parameters (force constants, etc.) were assumed for the vibrational modes to model the two species in binary liquid mixture, and were assigned according to specified mole fractions. Specific values of the parameters assumed in the present calculation are summarized in Table I.

Ensembles of liquid structures of a 512-particle system, with respect to the locations and orientations of the particles, were generated by the Monte Carlo method.[36] Two thermodynamic states, (T^*, ρ^*) = (2.0, 0.9) and (4.0, 0.45) (called state A and B hereafter),[35] where T^* ($\equiv T/\varepsilon$) and ρ^* ($\equiv\rho\sigma^3$) are the reduced temperature and density, were considered as examples. To simulate preferential solvation in this binary liquid mixture, *virtual energy of self association* (VESA), which is a separate energy scale and operates between the molecules of the same species within the first solvation layer, was introduced in the assignment of the parameters of vibrational modes, and ensembles of the assignments were generated by the Monte Carlo method on the basis of the sum of this virtual energy. In other words, simulations of the liquid structures were carried out in two steps:

TABLE I. Values of the parameters of vibrational modes assumed in the present calculation.

	Species 1	Species 2
force constant (mdyn Å^{-1} amu^{-1})[a]		
average[b]	1.7	1.1
standard deviation[c]	0.017	0.011
$\lvert\partial\boldsymbol{\mu}_m/\partial q_m\rvert$ (D Å^{-1} amu$^{-1/2}$)[d]	1.5	1.21
$(\partial\boldsymbol{\alpha}_m/\partial q_m)_{zz}$ (arbitrary unit)[e]	1.0	1.0

[a] Weighted by the inverse of the mass.

[b] Corresponding to the uncoupled vibrational frequencies of 1698.6 and 1366.4 cm^{-1}.

[c] Gaussian distribution is assumed.

[d] The direction of $\partial\boldsymbol{\mu}_m/\partial q_m$ is parallel to the permanent dipole of each particle.

[e] The form of $\partial\boldsymbol{\alpha}_m/\partial q_m$ is assumed to be axially symmetric, only its *zz* component being nonzero, where *z* axis is taken to be parallel to the permanent and transition dipoles.

locations and orientations of the particles were determined by the real interaction energy (determined by ε, σ, and μ), and for each set (configuration) of those locations and orientations of the particles, ensembles of the assignments of the molecular species were generated with a separate energy scale. Since the locations and orientations of the particles were fixed in the latter step, it is possible to examine the effect of preferential solvation on vibrational band profiles separately from those of the translational and rotational degrees of freedom of the liquid structures. In the present calculation, a few values of VESA were assumed as described below in section III. In total, 2500 sets of liquid structures were sampled for the calculation of the vibrational spectrum for each value of VESA and at each mole fraction.

The vibrational modes of different particles are coupled by the transition dipole coupling (TDC) mechanism,[23–26,28–31,33] expressed as

$$F_{mn} = -\frac{\partial\boldsymbol{\mu}_m}{\partial q_m}\cdot\boldsymbol{T}_{mn}\cdot\frac{\partial\boldsymbol{\mu}_n}{\partial q_n} \qquad (m \neq n) \qquad (1)$$

where $\boldsymbol{T}_{mn}$ is the dipole interaction tensor between the *m*th and *n*th particles, which is given as

$$\boldsymbol{T}_{mn} = \frac{3\boldsymbol{r}_{mn}\boldsymbol{r}_{mn} - r_{mn}^2\boldsymbol{I}}{r_{mn}^5} \qquad (2)$$

where $\boldsymbol{r}_{mn} = \boldsymbol{r}_m - \boldsymbol{r}_n$ is the distance vector (of length r_{mn}) between the particles, and $\boldsymbol{I}$ is a 3 × 3 unit tensor. TDC is known as the typical coupling mechanism for the vibrational modes exhibiting a large magnitude of NCE, e.g., the C=O stretching modes of many carbonyl compounds (such as acetone and *N*,*N*-dimethylformamide), the O–H and C–O stretching modes of methanol, the O–H stretching mode of water, and the S=O stretching mode of dimethyl sulfoxide. The normal modes of the liquid system were calculated by diagonalizing the vibrational Hamiltonian constructed from the force constants of individual oscillators (diagonal terms) and the vibrational couplings according to the TDC mechanism (off-diagonal terms). The IR and Raman spectra were calculated from those normal modes combined with the vibrational transition dipoles and the Raman tensors.[23]

The calculations described above were carried out with our original programs on Hewlett–Packard zx6000 and other servers. Part of the calculations was carried out on Altix 4700 computers at the Research Center for Computational Science of the National Institutes of Natural Sciences at Okazaki.

III. RESULTS AND DISCUSSION

As an example of the calculated radial distribution functions, those calculated for state A with $VESA_{11} = -0.4\ kT$ (operating between molecules of species 1) at the mole fraction $x_1 = 0.5$ are shown in the upper part of Fig. 1. It is seen that preferential solvation occurs between the molecules of the same species as a result of the VESA, so that the local mole fractions x_{11}^{L} and x_{22}^{L}, where x_{mn}^{L} is defined as the mole fraction of species m in the surroundings (the first solvation layer) of a molecule of species n,[1] are larger than the (global) mole fractions x_1 and x_2 (= 0.5). In this case, microscopic inhomogeneity extends to the second solvation layer. The small steps of the radial distribution functions at $r = 6.22$ Å are the artifacts due to the modeling of preferential solvation described above, but will be smoothed by defining the VESA as decreasing gradually as r increases rather than vanishing suddenly at the boundary of the first solvation layer ($r = 6.22$ Å) as in the present calculation. The IR and Raman spectra calculated for this case are shown in the lower part of Fig. 1. In both the frequency regions of the vibrations of species 1 (~1700 cm^{-1}) and species 2 (~1360 cm^{-1}), the isotropic Raman band is lower in frequency than the IR and anisotropic Raman bands (the NCE). At the same time, the isotropic Raman band profiles are noticeably asymmetric. Both the NCE and the asymmetry of the band profiles originate from the vibrational couplings. Although the band asymmetry is also informative of intermolecular interactions,[37] only the behavior of the NCE is discussed in the present work. In the presence of band asymmetry, the peak positions and the first moments are different. In such a case, it is legitimate to evaluate the value of NCE (defined as $\tilde{\nu}_{NCE(aniso\text{-}iso)} \equiv \tilde{\nu}_{aniso} - \tilde{\nu}_{iso}$ and $\tilde{\nu}_{NCE(IR\text{-}iso)} \equiv \tilde{\nu}_{IR} - \tilde{\nu}_{iso}$) on the basis of the first moments.[38]

The concentration dependencies of the relative magnitudes of NCE and the local mole fractions x_{11}^{L} and x_{22}^{L} calculated for a few values of VESA are shown in Fig. 2. The former quantity is defined, for the vibrational band of each species,

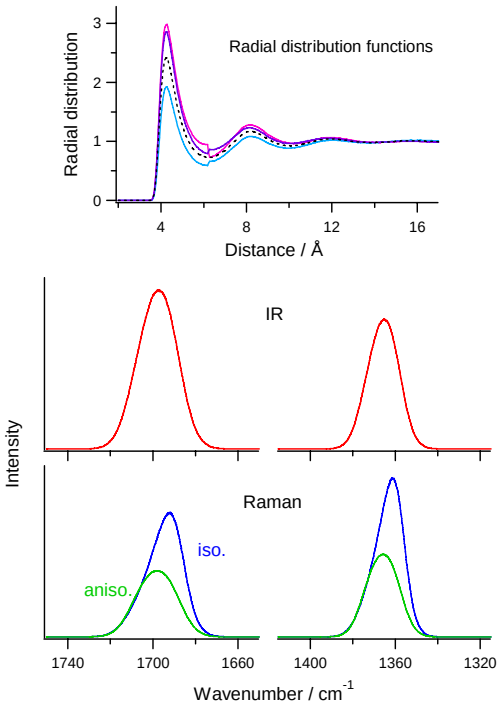

FIG. 1. Radial distribution functions (upper part) and the IR and Raman spectra (lower part) calculated for state A with $VESA_{11} = -0.4\ kT$ (operating between molecules of species 1) at the mole fraction $x_1 = 0.5$, taken as an example. In the upper part, $g_{11}(r)$, $g_{22}(r)$, and $g_{12}(r)$ (where $g_{mn}(r)$ is the function for the distances between the molecules of species m and species n) are shown in pink, purple, and light blue, respectively. The function in the case of no preferential solvation is shown with a black broken line as a reference. In the Raman spectra (bottom), the isotropic and anisotropic components are shown in blue and green, respectively.

as the value of NCE ($\tilde{\nu}_{NCE(aniso\text{-}iso)}$ or $\tilde{\nu}_{NCE(IR\text{-}iso)}$) at a specified mole fraction divided by that of the neat liquid. In the case of no preferential solvation, the relative magnitudes of NCE depend linearly on the mole fraction. However, as the preferential solvation is introduced by VESA, the concentration dependencies of the relative magnitudes of NCE of both species become convex, in the same way as those of the local mole fractions. As expected, the deviation is largest at intermediate concentrations. In the case of state A, the calculated behavior of $\tilde{\nu}_{NCE(IR\text{-}iso)}$ is indistinguishable from that of $\tilde{\nu}_{NCE(aniso\text{-}iso)}$ (overlapped in Fig. 2), and is almost symmetric between the vibrational bands of species 1 and 2. In the case of state B, however, the behavior of $\tilde{\nu}_{NCE(IR\text{-}iso)}$ and $\tilde{\nu}_{NCE(aniso\text{-}iso)}$

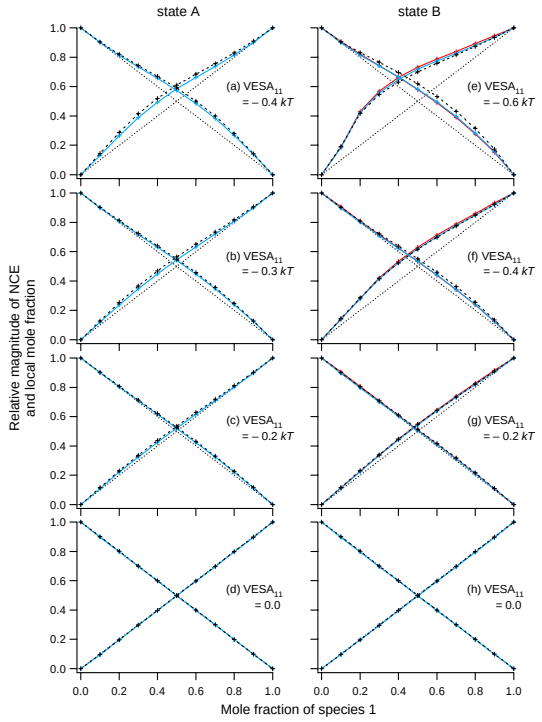

FIG. 2. Concentration dependencies of the relative magnitudes of NCE of the vibrational bands of species 1 and 2 (color lines) and the local mole fractions x_{11}^{L} and x_{22}^{L} (black broken lines) calculated for state A (left, a–d) and state B (right, e–h) with the values of VESA specified in each part. For state B, the curves for $\tilde{\nu}_{\mathrm{NCE(IR\text{-}iso)}}$ (red) do not overlap with those of $\tilde{\nu}_{\mathrm{NCE(aniso\text{-}iso)}}$ (light blue), so that they are drawn separately. The black dotted lines indicate linear dependencies and are drawn as a reference.

of the vibrational bands of species 1 and 2 is noticeably asymmetric, with the deviation from the linear behavior being larger for the vibrational band of species 1. This is probably because of the rather low density (ρ^*) of this state. Note that the VESA is introduced only between the molecules of species 1 in the present calculation. In spite of this asymmetry, when the magnitude of VESA is sufficiently large, the convex dependence of the NCE is recognized for the vibrational band of species 2 as well as that of species 1.

As predicted in a previous theoretical study based on the mean spherical approximation of liquid structures[28] and confirmed experimentally,[31] nonlinear dependencies of the relative magnitudes of NCE on the mole fraction are also seen when the molecules of the two species in a binary liquid mixture have different polarities (i.e., different magnitudes of dipole moments), because of the

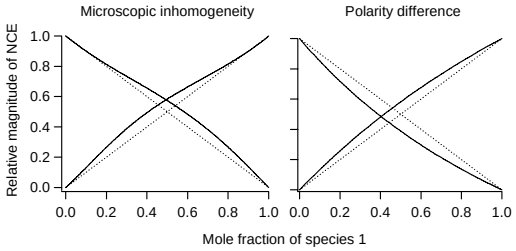

FIG. 3. Schematic drawings of the nonlinear concentration dependencies of the relative magnitudes of NCE arising from microscopic inhomogeneity (left) and polarity difference (right). The former is taken from Fig. 2 (a). The latter is drawn on the basis of Logan's theory [Eq. (17) of Ref. 28], assuming that the magnitude square of the dipole moment of species 1 is (as an example) twice as large as that of species 2.

molecular orientational effect on the magnitude of NCE. However, these nonlinear dependencies are distinguished from those arising from microscopic inhomogeneity, as shown schematically in Fig. 3. In the case of polarity difference, the behavior of the NCE of the more polar species exhibits a convex curvature, while that of the less polar species exhibits a concave curvature.[28] This means that, when the NCEs of the vibrational bands of both species are observed, one of them shows a convex curvature and the other shows a concave curvature, as shown on the right-hand side of Fig. 3, which is drawn by assuming that the magnitude square of the dipole moment of species 1 is (as an example) twice as large as that of species 2 in Eq. (17) of Ref. 28. This is distinguished from the situation arising from microscopic inhomogeneity shown on the left-hand side of Fig. 3, where the NCEs of the vibrational bands of both species show convex curvatures.

In real binary liquid mixtures, the molecular dipole moments of the two species are generally different, so that the factors shown in both parts of Fig. 3 should be simultaneously taken into account. It should be noted that only the molecular orientational effect arising from polarity difference (and no effect of microscopic inhomogeneity) is involved in the behavior on the right-hand side of Fig. 3, as clearly recognized from the derivation of Eq. (17) in Ref. 28, while only the effect of microscopic inhomogeneity (and no effect of polarity difference) is involved in the behavior on

the left-hand side of Fig. 3. In this sense, it is important to analyze the behavior of the NCEs of the vibrational bands of both species in the liquid mixture, especially that of the less polar species, to discuss the extent of microscopic inhomogeneity. Observation of convex behavior of the NCEs for the vibrational bands of both species will be a clear indication of the occurrence of microscopic inhomogeneity.

Acknowledgment

This study was supported by a Grant-in-Aid for Scientific Research from the Ministry of Education, Culture, Sports, Science, and Technology of Japan, and by a grant from the Morino Foundation for Molecular Science.

References

[1] Y. Marcus, *Solvent Mixtures* (Marcel Dekker, New York, 2002).
[2] J. G. Kirkwood and F. P. Buff, J. Chem. Phys. **19**, 774 (1951).
[3] A. Ben-Naim, J. Chem. Phys. **67**, 4884 (1977).
[4] E. Matteoli, J. Mol. Liq. **79**, 101 (1999).
[5] E. v. Goldammer and H. G. Hertz, J. Phys. Chem. **74**, 3734 (1970).
[6] Y. Marcus and Y. Migron, J. Phys. Chem. **95**, 400 (1991).
[7] K. Nishikawa, H. Hayashi, and T. Iijima, J. Phys. Chem. **93**, 6559 (1989).
[8] T. Takamuku, M. Tabata, M. Kumamoto, A. Yamaguchi, J. Nishimoto, H. Wakita, and T. Yamaguchi, J. Phys. Chem. B **102**, 8880 (1998).
[9] K. Yoshida, T. Yamaguchi, T. Otomo, M. Nagao, H. Seto, and T. Takeda, J. Mol. Liq. **119**, 125 (2005).
[10] M. Misawa, J. Phys. Soc. Jpn. **72**, 185 (2003).
[11] D. T. Bowron, J. L. Finney, and A. K. Soper, J. Phys. Chem. B **102**, 3551 (1998).
[12] J. E. Bertie and Z. Lan, J. Phys. Chem. B **101**, 4111 (1997).
[13] J. R. Reimers and L. E. Hall, J. Am. Chem. Soc. **121**, 3730 (1999).
[14] K. Egashira and N. Nishi, J. Phys. Chem. B **102**, 4054 (1998).
[15] S. Schrödle, B. Fischer, H. Helm, and R. Buchner, J. Phys. Chem. A **111**, 2043 (2007)
[16] D. S. Venables and C. A. Schmuttenmaer, J. Chem. Phys. **113**, 11222 (2000).
[17] H. Kovacs and A. Laaksonen, J. Am. Chem. Soc. **113**, 5596 (1991).
[18] R. D. Mountain, J. Phys. Chem. A **103**, 10744 (1999).
[19] K. Yoshida, T. Yamaguchi, A. Kovalenko, and F. Hirata, J. Phys. Chem. B **106**, 5042 (2002).
[20] K. Yoshida and T. Yamaguchi, Z. Naturforsch. **56a**, 529 (2001).
[21] T. Takamuku, T. Yamaguchi, M. Asato, M. Matsumoto, and N. Nishi, Z. Naturforsch. **55a**, 513 (2000).
[22] S. Dixit, J. Crain, W. C. K. Poon, J. L. Finney, and A. K. Soper, Nature **416**, 829 (2002).
[23] H. Torii, in *Novel Approaches to the Structure and Dynamics of Liquids: Experiments, Theories and Simulations*; edited by J. Samios and V. A. Durov (Kluwer, Dordrecht, The Netherlands, 2004), pp. 343–360.
[24] H. Torii, M. Musso, and M. G. Giorgini, J. Phys. Chem. A **109**, 7797 (2005).
[25] H. Torii, J. Phys. Chem. A **110**, 4822 (2006).
[26] H. Torii, J. Phys. Chem. A **110**, 9469 (2006).
[27] G. Fini, P. Mirone, and B. Fortunato, J. Chem. Soc. Faraday Trans. 2, **69**, 1243 (1973).
[28] D. E. Logan, Chem. Phys. **131**, 199 (1989).
[29] H. Torii and M. Tasumi, J. Chem. Phys. **99**, 8459 (1993).
[30] M. Musso, H. Torii, P. Ottaviani A. Asenbaum, and M. G. Giorgini, J. Phys. Chem. A **106**, 10152 (2002).
[31] M. Musso, M. G. Giorgini, H. Torii, R. Dorka, D. Schiel, A. Asenbaum, D. Keutel, and K.-L. Oehme, J. Mol. Liq. **125**, 115 (2006).
[32] R. Schweitzer-Stenner, F. Eker, K. Griebenow, X. Cao, and L. A. Nafie, J. Am. Chem. Soc. **126**, 2768 (2004).
[33] H. Torii, J. Phys. Chem. B **111**, 5434 (2007).
[34] J.-P. Hansen and I. R. McDonald, *Theory of Simple Liquids* (Academic Press, London, 1986).
[35] H. Torii, J. Phys. Chem. A **108**, 2103 (2004).
[36] M. P. Allen and D. J. Tildesley, *Computer Simulation of Liquids* (Oxford University Press, Oxford, 1989).
[37] M. Musso, H. Torii, M. G. Giorgini, and G. Döge, J. Chem. Phys. **110**, 10076 (1999).
[38] M. Musso, M. G. Giorgini, G. Döge, and A. Asenbaum, Mol. Phys. **92**, 97 (1997).